DOI: 10.1002/anie.200806208

Mesoporous Materials

Simple Synthesis of Graphitic Ordered Mesoporous Carbon Materials by a Solid-State Method Using Metal Phthalocyanines**

*Kyu Tae Lee, Xiulei Ji, Mathieu Rault, and Linda F. Nazar**

Mesoporous materials with high surface area, large pore volume, optimal pore size, and a precisely ordered pore structure are highly attractive for applications in energy conversion and storage devices.[1] In particular, ordered mesoporous carbon materials are promising as the supporting matrix for catalysts in fuel cells,[1a,2] hydrogen storage materials,[3] electrochemical double-layer capacitors,[4] and electrode materials in lithium batteries.[5] After the report of the first such carbon-based material in 1999 by Ryoo et al., a multitude of mesoporous carbon materials have been synthesized using the inverse replica technique, which is based on impregnating mesoporous silicates with a soluble or fluid carbon precursor.[6] However, this method is not amenable to larger scale-up. It thus limits the practicality of ordered mesoporous carbon materials, even though they show superior properties to their disordered analogues. Therefore, development of a synthetic method that utilizes a simple procedure is one of the important challenges in this field. Moreover, the framework of most carbon replica materials has an amorphous structure with relatively low electrical conductivity and poor mechanical strength, resulting in much inferior electrochemical performance compared to graphitic carbon materials.[2b,7]

Several synthetic routes to graphitic ordered mesoporous carbon materials have been reported. High-temperature methods using various carbon sources were found to lead to collapse of the pore structure[8] unless aromatic precursors such as pitches or benzene were employed. Ordered mesoporous carbon materials with a semigraphitic wall structure have been synthesized at relatively low temperatures by these methods. Nonetheless, the method is limited by the many complicated process steps required to impregnate the fluid precursor.[9] Catalytic graphitization and chemical vapor deposition (CVD) methods are also successful in synthesizing graphitic ordered mesoporous carbon.[10,11] However, both are cumbersome. The former requires an additional catalyst impregnation step, and the latter necessitates prior surface modification of the silica template (Al-doped SBA-15) to bind the carbon. A simpler CVD method that does not use a specialized autoclave was recently introduced.[2b,12] This method uses a conventional furnace with carbon precursor gases diluted in flowing inert gas. Only very low yields can be obtained. Carbon precursor gases can only be deposited on the silica template when they make contact, and most of the precursor gases exit without reaction. Hence the carbon yield is less than about 5 wt%, for example, when ferrocene is used as a carbon precursor.[2b] Furthermore, the degree of graphitization of most mesoporous carbon materials obtained from CVD methods without additional catalytic graphitization is not very high, and the surface area and pore volume of these carbon materials are relatively low. Herein, we introduce a facile, one-step route for the synthesis of highly graphitic ordered mesoporous carbon (CMK-3) with high surface area and pore volume using a pseudo-solid-state method involving metal phthalocyanines (MPc) and SBA-15. This synthesis is strategically combined with in situ chemical vapor deposition and catalytic graphitization.

The process is very simple. Nickel phthalocyanine and ordered mesoporous silica (SBA-15) were ground together in a 1:1 weight ratio. The powders were heated at 900 °C in a tube furnace under Ar flow, and the resultant carbon–silica composites were treated with a HF solution to dissolve the silica. The resulting product (CMK-3-NiPc) shows a highly ordered pore structure (Figure 1). The TEM image for the (110) plane shows ideal hexagonal close packing of the carbon rods (Figure 1a). The TEM image corresponding to the (001) plane also exhibits a highly ordered pore structure, which is well-developed throughout the entire particle (Figure 1b). The fact that the particle size (ca. 700 nm) and morphology of

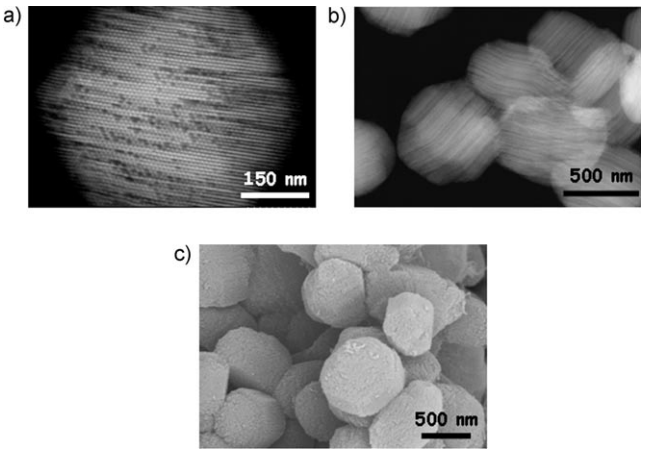

Figure 1. TEM images for a) the (110) plane and b) the (001) plane of CMK-3-NiPc, and c) SEM image of CMK-3-NiPc. The dark spots in (a) indicate defects (empty sites) in the hexagonal close-packed carbon-rod structure.

[*] Dr. K. T. Lee, X. Ji, M. Rault, Prof. L. F. Nazar
Department of Chemistry, University of Waterloo
Waterloo, ON, N2L 3G1 (Canada)
Fax: (+1) 519-746-0435
E-mail: lfnazar@uwaterloo.ca

[**] NSERC is gratefully acknowledged for financial support. We thank Dr. Neil Coombs, University of Toronto, for help with acquisition of the TEM images.

Supporting information for this article is available on the WWW under http://dx.doi.org/10.1002/anie.200806208.

CMK-3-NiPc are exactly same as those of SBA-15 (Figure 1c) shows that the carbon is a faithful inverse replica of the silica at all length scales. Low-angle X-ray diffraction (XRD) patterns display reflections typical of ordered mesoporous carbon (Figure 2a).

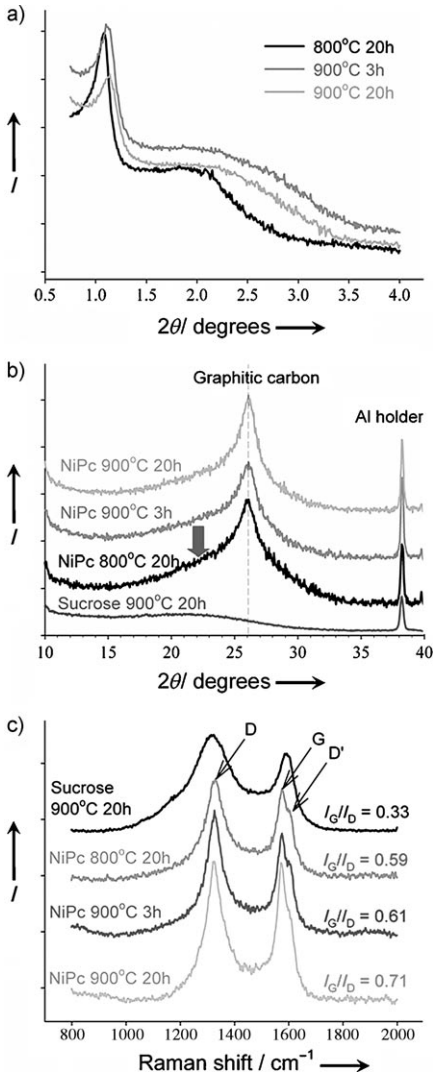

Figure 2. Effect of heat treatment on crystallinity and pore structure of CMK-3. a) Small-angle and b) wide-angle XRD patterns as well as c) Raman spectra of the CMK-3-NiPc materials obtained at various temperatures. The arrow in (b) highlights the broad peak corresponding to amorphous carbon.

Significant is that CMK-3-NiPc has a more highly graphitic wall structure than typical CMK-3 obtained by the conventional impregnation method using sucrose as a carbon source (Figure 2b and c). We further varied the pyrolysis temperature and time to optimize the degree of graphitization. When CMK-3-NiPc was heated at 800 °C for 20 h, the product is composed of both graphitic carbon and amorphous carbon. The sharp peak at 26° and broad peak at approximately 22° (arrow) in Figure 2b are representative of the graphitic carbon and amorphous carbon contributions, respectively. However, with increasing pyrolysis temperature and time, the intensity of the broad peak near 22° gradually diminishes. Highly graphitic CMK-3-NiPc was obtained by pyrolysis at 900 °C for 20 h; no pore collapse was detected. The coherence length (L_c) along [001] was 4.9 nm (a very long length scale for a mesoporous wall structure), and the d spacing of the (002) peak (corresponding to the interlayer distance) is 3.41 Å, which is only slightly larger than that of pure graphite (3.354 Å). This is the strongest evidence for the highly graphitic nature of CMK-3-NiPc, as L_c increases and the d spacing decreases as the degree of graphitization increases.[13] The graphitic wall structure of NiPc carbon materials is also evident in the Raman spectra shown in Figure 2c. The G band at 1570 cm^{-1} arising from in-plane stretching is noticeably sharper and the intensity ratio of G band to D band is much higher than for nongraphitic CMK-3 (sucrose). The shoulder (D′) at 1600 cm^{-1} is attributed to the defect structure of nanocrystalline graphite, as explained in previous studies that elucidate the origin of this feature.[14] With increasing pyrolysis temperature and time, the D′ peak gradually diminishes, meaning that the degree of graphitization increases. This finding is consistent with XRD data. The surface area, pore volume, and pore diameter of CMK-3-NiPc are 1122 m^{2}g^{-1}, 1.17 cm^{3}g^{-1}, and 3.1 nm, respectively. These values are slightly lower than those of typical CMK-3 that possesses amorphous walls but are much higher than those of graphitic CMK-3 reported elsewhere (Table 1). As the pyrolysis temperature and time are increased, the pore size slightly decreases, as shown in Figure 3. This trend is confirmed by low-angle XRD (Figure 2a), which shows a shift in the peak position to higher values with increased temperature.

Above all, it is important to note that the carbon yields are around 70–75 wt %, which is more than an order of magnitude higher than those of carbon materials obtained from the other CVD methods. It is known that metal phthalocyanines characteristically sublime near 500 °C.[15] However, they decompose into carbon when heated at just above their

Table 1: Surface area, pore volume, and pore size of CMK-3-MPc materials (M = Ni, Fe, Co, Mn) and other referenced CMK-3 materials.

CMK-3 from various carbon precursors or methods	Surface area [m^{2}g^{-1}]	Pore volume [cm^{3}g^{-1}]	Pore size[a] [nm]	d_{200} [Å]	L_c [nm]
NiPc 900 °C 20 h	1122	1.17	3.1	3.41	4.9
NiPc 900 °C 3 h	1107	1.01	3.1	3.42	–
NiPc 800 °C 20 h	1022	0.93	3.4	3.42	–
FePc 900 °C 3 h	877	0.75	2.8	3.45	4.3
CoPc 900 °C 3 h	602	0.93	2.2	3.44	4.3
MnPc 900 °C 3 h	1160	0.90	1.9	–	–
sucrose[b]	1261	1.56	3.8	–	–
pitch (*P6mm*)[c]	390	0.43	3.68	3.5	–
CMK-3Va[d]	678	0.70	–	–	–
CCVD 3.5 h[e]	661	0.81	2.94	–	–
Ni DGMC[f]	799	0.73	3.23	3.53	–
C_{bzn}[g]	685	1.00	2.4	–	–

[a] Peak pore size in BJH adsorption pore size distribution. [b] CMK-3 with amorphous walls prepared by a conventional impregnation method using sucrose with heating at 900 °C for 20 h. [c] Ref. [9b]. [d] CVD; Ref. [12]. [e] Catalytic CVD; Ref. [10b]. [f] Ni-catalysed graphitization; Ref. [10a]. [g] Benzene source; Ref. [9a].

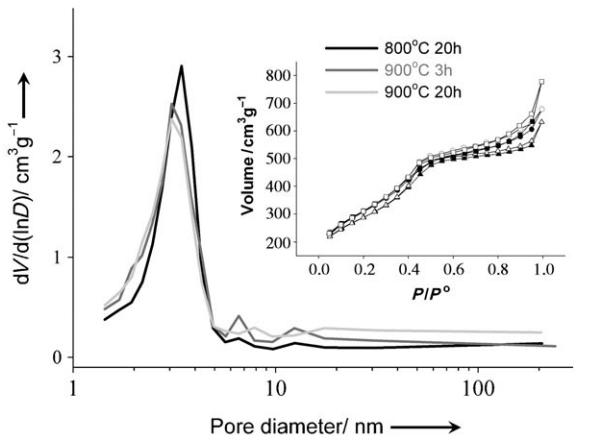

Figure 3. Barrett–Joyner–Halenda (BJH) adsorption pore-size distribution and nitrogen adsorption–desorption isotherms (inset; ▲, △ 800 °C, 20 h; ●, ○ 900 °C, 3 h; ■, □ 900 °C, 20 h; filled symbols are adsorption, empty ones are desorption) of the CMK-3-NiPc materials obtained under different pyrolysis conditions.

sublimation temperature under an inert-gas atmosphere. In fact, they have been used to coat carbon on metal nanoparticles and to synthesize carbon nanotubes.[16] The carbon yields are usually 70–85 wt %, even though the inert carrier gas and phthalocyanine vapor flow continuously through the furnace.[15,16] This means that the sublimation and decomposition temperatures of metal phthalocyanines must be quite similar; that is, these events occur almost simultaneously during the heat-treatment process. Therefore, when the mixed powders of nickel phthalocyanine and SBA-15 are heated in our synthesis, nickel phthalocyanine is sublimed and semi-graphitic carbon is almost instantaneously coated on the surface of SBA-15. This process occurs homogeneously, resulting in a very well-ordered pore structure (Figures 1 and 2 a). This pore structure seems to be the result of a short diffusion path of the sublimed nickel phthalocyanines during thermal treatment, because nickel phthalocyanine and SBA-15 are mixed on a very small length scale. Therefore, we term this a pseudo-solid-state method. We expect that this approach should be very suitable for bulk production of graphitic ordered mesoporous carbon materials. The procedure is as simple as many of the commercialized solid-state methods to produce inorganic powders.

After heating nickel phthalocyanine and SBA-15, the obtained powders are comprised of nickel nanoparticles dispersed in the graphitic CMK-3 and SBA-15 composites. Nickel metal is known to be a very efficient catalyst for graphitization. Therefore, the highly graphitic structure of CMK-3-NiPc undoubtedly originates from this "in situ" catalyst source. Along these lines, other metal phthalocyanines (M = Fe, Co, Mn) were examined to compare their catalytic effects on graphitization. Ordered graphitic mesoporous carbon materials similar to CMK-3-NiPc were obtained from iron and cobalt phthalocyanines (CMK-3-FePc, CMK-3-CoPc), but the degree of graphitization of CMK-3-MnPc obtained from the manganese precursor was not as high as that in carbon materials from other metal phthalocyanines (Figure 4). This result is not surprising, as it is well known that Ni, Fe, and Co are most effective for this catalytic process. We note that the surface area and pore volume of CMK-3-FePc and CMK-3-CoPc were less than those of CMK-3-NiPc (Table 1). We believe that this effect is due to the different temperature and rate of sublimation or decomposition of the different metal phthalocyanines.

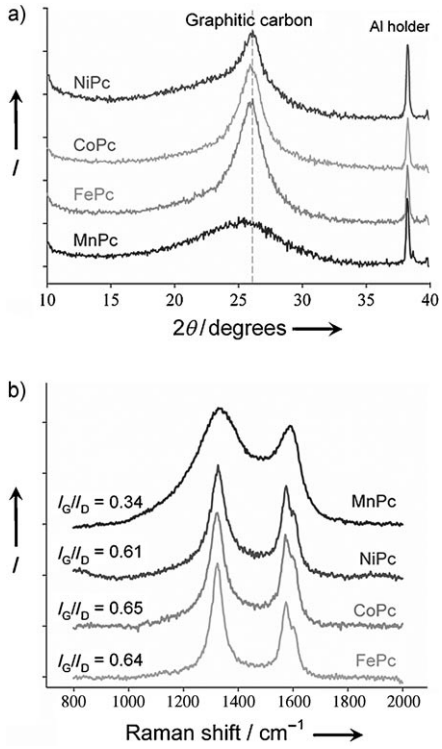

Figure 4. a) XRD patterns and b) Raman spectra of various CMK-3-MPc materials heated at 900 °C for 3 h (M = Ni, Co, Fe, Mn).

Furthermore, metal nanoparticles dispersed in graphitic mesoporous carbon materials can be obtained by using base (NaOH) instead of HF to dissolve the silica template. In the latter case both metal and silica are dissolved, as for CMK-3-FePc. However, when a basic solution is used, only SBA-15 is dissolved. Thus for CMK-3-FePc, iron nanoparticles with a size of approximately 5–20 nm were retained within the mesoporous structure (Figure 5 a), although some large agglomerated particles were also found. Iron metal was identified by energy-dispersive X-ray spectroscopy (EDS) line profiles (Figure 5 b). Weak silicon profiles were also detected, caused by trace amounts of SBA-15 that was not fully dissolved in the NaOH solution. Recently, a similar approach was used to synthesize copper–sulfur compounds dispersed in mesoporous carbon by an impregnation method using a water-soluble copper phthalocyanine tetrasulfonic acid tetrasodium salt.[17] However, this mesoporous carbon material is not semi-graphitic and does not possess a highly ordered porous structure. Furthermore, the method requires complicated processes such as repeated impregnation of the precursor and subsequent HCl treatment. Our approach to directly synthesize metal nanoparticles dispersed within

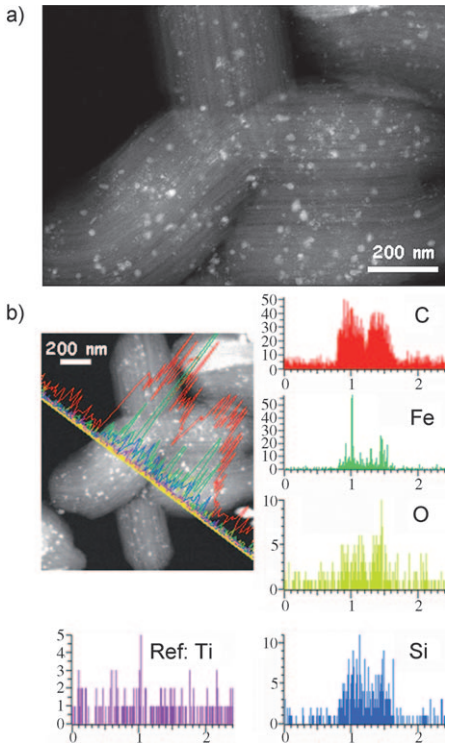

Figure 5. a) TEM image and b) EDS line profiles of the Fe-loaded graphitic CMK-3 obtained from iron phthalocyanine. *x* axes: distance [μm], *y* axes: X-ray intensity.

graphitic mesoporous carbon materials can be easily extended to platinum and ruthenium phthalocyanines or to mixtures of transition-metal (Fe, Co, Ni) and platinum phthalocyanines to form binary alloy nanoparticles. These materials have very promising properties as catalysts for both proton exchange membrane fuel cells (PEMFCs) and direct formic acid fuel cells as compared to pure Pt-loaded CMK-3,[1a] and work is ongoing in our laboratory to explore these properties.[18]

One important consideration for fuel-cell applications is the stability of the carbon material towards electrochemical oxidation. Most porous carbon materials used as catalyst supports can suffer oxidation, which affects the long-term durability of PEMFCs. Degradation of the carbonaceous catalyst support causes electrical isolation of catalysts as well as decreasing gas permeability owing to the increased hydrophilic surface.[19] Highly graphitized carbon materials, which are more resistant to oxidation,[20] are very desirable if high pore volumes can also be attained. The electrochemical measurements of CMK-3-NiPc (20 h) and of a amorphous carbon material (sucrose precursor) are displayed in Figure 6. The first cycle compares the double-layer capacitor properties of the two materials using cyclic voltammograms acquired in 0.5 M H_2SO_4. CMK-3-NiPc exhibits a capacitance value of 130 $F g^{-1}$, comparable to the best ordered mesoporous carbon materials and 20% higher than the sucrose-derived CMK-3. It is far superior to highly graphitized CMK-3 materials derived from anthracence, for example, which display values of 20–60 $F g^{-1}$.[21] The voltammogram recorded after electrochemical oxidation in aqueous H_2SO_4 at 80 °C shows that the stability of CMK-3-NiPc is substantially enhanced versus the

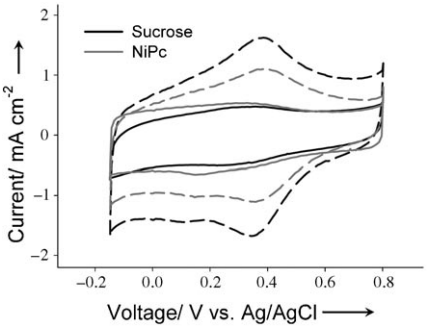

Figure 6. Cyclic voltammograms of CMK-3 carbon electrodes before (solid line) and after (dashed line) an electrochemical oxidation at 1.2 V (vs. standard hydrogen electrode) at 80 °C for 6 h. Scan rate = 20 $mV s^{-1}$; electrolyte = 0.5 M H_2SO_4.

amorphous carbon material. The peak at 0.35 V (vs. Ag/AgCl) is due to the hydroquinone–quinone redox couple of the oxidized carbon surface. The integrated current response is about half that of CMK-3-sucrose, owing to the much lower degree of surface oxidation.[20,22] These results will be described in detail elsewhere.

In summary, highly graphitic ordered mesoporous carbon materials have been synthesized by a simple pseudo-solid-state method employing metal pthalocyanines and SBA-15. The graphitic ordered mesoporous carbon materials have nanodomain graphitic pore walls with a d_{200} value of (3.42 ± 0.02) Å and about 4–5 nm domain size. They maintain a highly ordered 3 nm pore structure, exhibiting surface areas up to 1120 $m^2 g^{-1}$ upon treatment at 900 °C. The degree of graphitization is enhanced by the combined effect of catalytic graphitization and chemical vapor deposition. The pore structure remains completely intact upon heat treatment even though the wall is highly graphitic, and therefore these carbon materials exhibit very high surface areas and pore volumes as well as good oxidative stability and capacitance. Above all, this synthetic route is, to our knowledge, the most convenient and simplest way to obtain graphitic ordered mesoporous carbon materials.

Experimental Section

Synthesis of SBA-15: Surfactant P123 (12 g) was mixed in aqueous HCl (2 M, 360 mL) and water (300 mL). The mixture was stirred in an oven at 38 °C for 12 h until the surfactant was completely solubilized. Tetraethyl orthosilicate (TEOS, 25.2 g) was added; the mixture was vigorously stirred for 8 min and then placed in an oven at 38 °C overnight. The temperature was increased to 100 °C for 24 h. The product was filtered, dried, and calcined at 550 °C for 5 h to remove the surfactant.

Synthesis of CMK-3 by conventional impregnation: SBA-15 (1 g) was added to a solution obtained by dissolving sucrose (1.25 g) and concentrated H_2SO_4 (0.145 g) in H_2O (5 g). The mixture was placed in an ultrasonicator for 1 h and then in an oven at 100 °C for 12 h and 160 °C for 24 h. The solid was treated again with sucrose (0.8 g), conentrated H_2SO_4 (0.09 g), and H_2O (5 g) and heated at 100 °C (12 h) and 160 °C (24 h). The mixture was finally heated at 900 °C for 20 h in an Ar atmosphere. The resultant carbon–silica sample was washed with aqueous hydrofluoric acid (10 wt%) to remove the silica.

Synthesis of CMK-3-MPc by the pseudo-solid-state method: Metal phthalocyanine (2 g, metal = Ni, Fe, Co, Mn) and SBA-15 (2 g) were mixed using a mortar. The mixture was heated at 800 or 900 °C in an Ar atmosphere. The resultant carbon–silica composite was washed with aqueous hydrofluoric acid (10 wt %) to remove the silica. To synthesize iron nanoparticles dispersed in the mesoporous graphitic carbon material, the sample was washed with 1 M NaOH dissolved in a 1:1 mixture of water and ethanol at 80 °C.

Characterization: The ordered pore structure of the graphitic ordered mesoporous carbon materials was examined by transmission electron microscopy (TEM) using a Hitachi HD-2000 STEM instrument. Scanning electron microscopy (SEM) was carried out on a LEO 1530 field emission SEM instrument. X-ray diffraction patterns were collected on a D8-ADVANCE powder X-ray diffractometer operating at 40 kV and 30 mA and employing $Cu_{K\alpha}$ radiation ($\lambda =$ 0.15406 nm). Nitrogen adsorption and desorption isotherms were determined employing a Micromeritics Gemini 2735 system at −196 °C. The Raman spectra were recorded with a Renishaw 1000 spectrometer using a 632.8 nm He–Ne laser operating at 2 mW.

Electrochemical studies: The electrochemical oxidation of the CMK-3 carbon electrodes was analyzed with a three-electrode configuration in N_2-saturated aqueous 0.5 M H_2SO_4. To prepare the working electrode, CMK-3 carbon materials were suspended in 2-propanol and transferred by pipette onto the surface of the glassy carbon disk electrode. The CMK-3-coated electrode surface was then dried, and a 2-propanol solution containing 1 wt % nafion was added. The loading of each sample was 0.2 mg cm^{-2}. The electrodes were soaked in the electrolyte for 1 day before electrochemical characterization to fully wet the surface. A platinum wire and Ag/AgCl electrode were used as the counter and reference electrodes, respectively. The current transients for electrochemical oxidation were recorded with a hold at 1.2 V vs. NHE at 80 °C for 6 h. Cyclic voltammetry was performed using a VMP-3 potentiostat in the potential range of 0.05 to 1.0 V (vs. NHE) with a scan rate of 20 mV s^{-1}.

Received: December 19, 2008
Revised: March 12, 2009
Published online: June 30, 2009

Keywords: heterogeneous catalysis · carbon · mesoporous materials · solid-state reactions

[1] a) S. H. Joo, S. J. Choi, I. Oh, J. Kwak, Z. Liu, O. Terasaki, R. Ryoo, *Nature* **2001**, *412*, 169 – 173; b) Q. Huo, D. I. Margolese, U Ciesla, P. feng, T. E. Gier, P. Sieger, R. Leon, P. M. Petroff, F. Schüth, G. D. Stucky, *Nature* **1994**, *368*, 317 – 321; c) P. T. Tanev, T. J. Pinnavaia, *Science* **1995**, *267*, 865 – 867; d) F. Jiao, K. M. Shaju, P. G. Bruce, *Angew. Chem.* **2005**, *117*, 6708 – 6711; *Angew. Chem. Int. Ed.* **2005**, *44*, 6550 – 6553.

[2] a) H. Chang, S. H. Joo, C. Park, *J. Mater. Chem.* **2007**, *17*, 3078 – 3088; b) Z. Lei, S. Bai, Y. Xiao, L. Dang, L. An, G. Zhang, Q. Xu, *J. Phys. Chem. C* **2008**, *112*, 722 – 731; c) J. H. Nam, Y. Y. Jang, Y. U. Kwon, J. D. Nam, *Electrochem. Commun.* **2004**, *6*, 737 – 741.

[3] Z. Yang, Y. Xia, R. Mokaya, *J. Am. Chem. Soc.* **2007**, *129*, 1673 – 1679.

[4] S. Yoon, J. Lee, T. Hyeon, S. M. Oh, *J. Electrochem. Soc.* **2000**, *147*, 2507 – 2512.

[5] a) H. Zhou, S. Zhu, M. Hibino, I. Honma, M. Ichihara, *Adv. Mater.* **2003**, *15*, 2107 – 2111; b) J. Fan, T. Wang, C. Yu, B. Tu, Z. Jiang, D. Zhao, *Adv. Mater.* **2004**, *16*, 1432 – 1436.

[6] R. Ryoo, S. H. Joo, S. Jun, *J. Phys. Chem. B* **1999**, *103*, 7743 – 7746.

[7] T. Hyeon, S. Han, Y. E. Sung, K. W. Park, Y. W. Kim, *Angew. Chem.* **2003**, *115*, 4488 – 4492; *Angew. Chem. Int. Ed.* **2003**, *42*, 4352 – 4356.

[8] A. B. Fuertes, S. Alvarez, *Carbon* **2004**, *42*, 3049 – 3055.

[9] a) C. H. Kim, D. K. Lee, T. J. Pinnazaia, *Langmuir* **2004**, *20*, 5157 – 5159; b) H. Yang, Y. Yan, Y. Liu, F. Zhang, R. Zhang, Y. Meng, M. Li, S. Xie, B. Tu, D. Zhao, *J. Phys. Chem. B* **2004**, *108*, 17320 – 17328.

[10] a) X. Ji, P. S. Herle, Y. Rho, L. F. Nazar, *Chem. Mater.* **2007**, *19*, 374 – 383; b) W. H. Zhang, C. Liang, H. Sun, Z. Shen, Y. Guan, P. Ying, C. Li, *Adv. Mater.* **2002**, *14*, 1776 – 1778.

[11] T. W. Kim, I. S. Park, R. Ryoo, *Angew. Chem.* **2003**, *115*, 4511 – 4515; *Angew. Chem. Int. Ed.* **2003**, *42*, 4375 – 4379.

[12] Y. Xia, R. Mokaya, *Adv. Mater.* **2004**, *16*, 1553 – 1558.

[13] I. Mochida, R. Fujiura, T. Kojima, H. Sakamoto, T. Yoshimura, *Carbon* **1995**, *33*, 265 – 274.

[14] a) A. C. Ferrari, J. Robertson, *Phys. Rev. B* **2000**, *61*, 14095 – 14107; b) A. C. Ferrari, *Solid State Commun.* **2007**, *143*, 47 – 57.

[15] B. N. Achar, G. M. Fohlen, J. A. Parker, *J. Polymer Sci. Polymer Chem. Ed.* **1982**, *20*, 1785 – 1790.

[16] a) K. T. Lee, Y. S. Yoon, T. Kim, C. H. Kim, J. H. Kim, J. Y. Kwon, S. M. Oh, *Electrochem. Solid-State Lett.* **2008**, *11*, A21 – A24; b) T. Kim, S. Park, S. M. Oh, *Electrochem. Commun.* **2006**, *8*, 1461 – 1467; c) N. S. Kim, Y. T. Lee, J. Park, J. B. Han, Y. S. Choi, S. Y. Choi, J. Choo, G. H. Lee, *J. Phys. Chem. B* **2003**, *107*, 9249 – 9255.

[17] A. H. Lu, H. Tuysuz, F. Schüth, *Microporous Mesoporous Mater.* **2008**, *111*, 117 – 123.

[18] X. Ji, K. T. Lee, R. Holden, L. Zhang, J. Zhang, L. F. Nazar, unpublished results.

[19] R. Borup et al., *Chem. Rev.* **2007**, *107*, 3904 – 3951 (see the Supporting Information).

[20] Y. Shao, G. Yin, J. Zhang, Y. Gao, *Electrochim. Acta* **2006**, *51*, 5853 – 5857.

[21] Y. Zhai, Y. Wan, Y. Cheng, Y. Shi, F. Zhang, B. Tu, D. Zhao, *J. Porous Mater.* **2008**, *15*, 601 – 611.

[22] a) S. C. Ball, S. L. Hudson, D. Thompsett, B. Theobald, *J. Power Sources* **2007**, *171*, 18 – 25; b) K. H. Kangasniemi, D. A. Condit, T. D. Jarvi, *J. Electrochem. Soc.* **2004**, *151*, E125 – E132.

